haematologica
Journal of the Ferrata Storti Foundation

Fibrinogen promotes acute myelogenous leukemia progression *via* miR-486/*GPR153* axis

by Ming Yang, Xiaofang You, Fan Zhao, Huida Tong, Haris Munir, Kaiwen Wu, Xiaomin Yu, Laixi Bi, Jie Xiang, Misheng Zhao, Shenghui Zhang, Chen Ling and Liqing Zhu

Received: April 28, 2025.
Accepted: April 27, 2026.

Citation: Ming Yang, Xiaofang You, Fan Zhao, Huida Tong, Haris Munir, Kaiwen Wu, Xiaomin Yu, Laixi Bi, Jie Xiang, Misheng Zhao, Shenghui Zhang, Chen Ling and Liqing Zhu. Fibrinogen promotes acute myelogenous leukemia progression via miR-486/GPR153 axis.
Haematologica. 2026 May 7. doi: 10.3324/haematol.2025.288109 [Epub ahead of print]

Fibrinogen promotes acute myelogenous leukemia progression *via* miR-486/*GPR153* axis

Ming Yang[1,2*], Xiaofang You[3*], Fan Zhao[4*], Huida Tong[1,5*], Haris Munir[1,2], Kaiwen Wu[5], Xiaomin Yu[5], Laixi Bi[6], Jie Xiang[5], Misheng Zhao[7#], Shenghui Zhang[4#], Chen Ling[1,2#], Liqing Zhu[3,5#]

[1]State Key Laboratory of Genetics and Development of Complex Phenotypes, School of Life Sciences, Zhongshan Hospital, Fudan University, Shanghai 200438, China

[2]Shanghai Key Laboratory of Gene Editing and Cell Therapy for Rare Diseases, Engineering Research Center of Gene Technology (Ministry of Education), Fudan University, Shanghai 200031, China

[3]Department of Clinical Laboratory, Peking University Cancer Hospital & Institute, Beijing 100142, China

[4]Department of Hematology and Laboratory Animal Center, The First Affiliated Hospital of Wenzhou Medical University, Wenzhou, Zhejiang 325000, China

[5]Department of Clinical Laboratory, the First Affiliated Hospital of Wenzhou Medical University, Wenzhou, Zhejiang 325000, China

[6]Department of Hematopathology, the First Affiliated Hospital of Wenzhou Medical University, Wenzhou, Zhejiang 325000, China

[7]Department of Blood Transfusion, Peking University Cancer Hospital & Institute, Beijing 100142, China

[*] **These authors contributed equally to this work.**

[#] **Correspondence should be addressed to**：

Liqing Zhu, Department of Clinical Laboratory, Peking University Cancer Hospital & Institute, Beijing 100142, China. zhuliqing@bjmu.edu.cn

Chen Ling, State Key Laboratory of Genetics and Development of Complex Phenotypes, School of Life Sciences, Zhongshan Hospital, Fudan University, Shanghai 200438, China. lingchenchina@fudan.edu.cn

Shenghui Zhang, Department of Hematology and Laboratory Animal Center, The First Affiliated Hospital of Wenzhou Medical University, Wenzhou, Zhejiang 325000, China. zhangshenghui@wmu.edu.cn

Misheng Zhao, Department of Blood Transfusion, Peking University Cancer Hospital & Institute, Beijing 100142, China. zhaomisheng@bjmu.edu.cn

Key words: Fibrinogen; AML; miR-486-5p; GPR153; mTORC2/AKT

Running title：Fibrinogen promotes AML progression via GPR153

Author contributions

M.Y., H.T., X.Y., F.Z. and K.W.: Investigation, Methodology, Visualization, Data curation, Formal analysis. X.Y., L.B., J.X., H.M., and M.Z.: Writing-original draft, Writing-review & editing. L.Z., C.L., and S.Z.: Conceptualization, Supervision, Resources, Funding acquisition, Writing-original draft, Writing-review & editing. All authors read and approved the final version of the manuscript.

Data availability statement: All of the data supporting this study's findings are available from the corresponding author.

Conflict of interest disclosure：The authors declare no conflicts of interest.

Ethics approval statement: All animal experiments were approved by Animal Care and Use Committee of the First Affiliated Hospital of Wenzhou Medical University.

Funding

This study was supported by the National Natural Science Foundation of China (Grant No. 82272784, to L.Z.), the Natural Science Foundation of Zhejiang Province (Grant No. LY22H200004, to L.Z.), the Zhejiang Province Science and Technology Plan Research and Xinmiao Talent Program (Grant No. 2023R413093, to H.T.), the Beijing High-Level Innovation and Entrepreneurship Talent Support Program Young Top Talent Projects (Grant No. 20250571).

Abstract

Acute myeloid leukemia (AML) is a frequently fatal malignancy of bone marrow stem/progenitor cells. Fibrinogen (Fg), the predominant coagulation factor in plasma, has been reported to have a negative correlation with the prognosis of AML patients. However, the underlying mechanisms through which Fg exerts its effects on AML remain unclear. In this study, we developed a Fg-deficient AML mouse model and utilized AML cell lines and primary human AML cells to explore the role of Fg in AML progression both *in vivo* and *in vitro*. Our findings demonstrate that Fg significantly accelerates AML progression in a cancer xenograft model, as well as primary cells from untreated patients with AML. Mechanistically, Fg upregulates the expression of miR-486-5p, which directly targets the orphan receptor GPR153. This interaction activates the downstream mTORC2/AKT signaling pathway, driving AML cell proliferation and migration. Our results highlight a critical molecular mechanism by which Fg contributes to AML progression, offering potential molecular targets for therapeutic intervention.

Key words: Fibrinogen; AML; miR-486-5p; GPR153; mTORC2/AKT

Introduction

Fibrinogen (Fg) is a glycoprotein synthesized by hepatocytes, which circulates in the bloodstream at concentrations of 2–4 g/L.[1] It plays a critical role in hemostasis by acting as a substrate for fibrin formation and binding to platelets to promote aggregation. Recently, it has been linked to the progression of solid tumors. For example, Fg enhances colorectal adenocarcinoma growth *via* activation of focal adhesion kinase (FAK) and protects melanoma and lymphoma cells from natural killer (NK) cell-mediated cytotoxicity by promoting platelet adhesion to tumor cells.[2, 3] Furthermore, Fg binds to VE-cadherin to facilitate the transendothelial migration of malignant epithelial cells in breast cancer.[4] Additionally, Fg supports angiogenesis by interacting with endothelial growth factors.[5]

The role of Fg in acute myeloid leukemia (AML) remains largely unexplored, despite its well-established function as an acute-phase protein involved in inflammation through interactions with leukocytes. Previous studies have predominantly focused on clinical data, identifying plasma Fg levels as a potential prognostic biomarker for treatment outcomes in AML.[6] Specifically, higher Fg levels at diagnosis are associated with poorer outcomes, including shorter overall survival (OS) and disease-free survival (DFS).[7, 8] Furthermore, the fibrinogen-albumin ratio index (FARI) has demonstrated a negative correlation with patient prognosis in AML.[9] These findings suggest that Fg may contribute to AML disease progression through unknown molecular mechanisms. It is of interest to investigate the underlying biology and potential therapeutic implications of Fg in AML.

The AKT/mTOR pathway is critical in leukemogenesis and AML progression, and is activated in 60–80% of AML patients[10]. This pathway promotes key oncogenic processes, including malignant cell proliferation, migration, and invasion. Targeting the AKT/mTOR pathway with inhibitors has been shown to impair bone marrow migration and improve survival outcomes in AML patients.[10, 11] G protein-coupled receptors (GPCRs), the largest and most diverse family of cellular receptors in eukaryotes, play essential roles in immune responses, neurotransmission, and other cellular processes.[12] Recently, GPCRs have been implicated in tumor initiation and progression, probably through the activation of multiple signaling pathways, including AKT/mTOR, MAPK, and Hippo.[13] However, the precise mechanisms through which GPCRs regulate the AKT/mTOR pathway in AML remain poorly understood.

In this manuscript, we developed a Fg-deficient AML mouse model and demonstrated that Fg accelerates AML progression by promoting the proliferation and migration of AML cells both in vitro and in vivo. Furthermore, RNA sequencing analysis revealed that Fg suppresses the expression of GPR153 while simultaneously activating the mTORC2/AKT pathway. We further validated that GPR153 down-regulation is mediated by miR-486-5p, and confirmed the functional link between GPR153 and the mTORC2/AKT pathway through knockdown and overexpression experiments. In summary, our findings uncover the role of Fg in AML progression and identify a novel miR-486-5p/GPR153/mTORC2/AKT pathway, which may offer a potential therapeutic target for future interventions.

Methods

Cell Culture

Primary embryonic human kidney cell line HEK293 and human or mouse AML cell lines THP-1 and C1498 were purchased from the American Type Culture Collection (ATCC, USA). Human AML cell line MV-4-11 was purchased from Shanghai Cell Biology Institute, Chinese Academy of Sciences. HEK293 and C1498 cells were cultured in complete Dulbecco's Modified Eagle's Medium (DMEM, Wisent Inc., Canada) containing 10% fetal bovine serum (FBS, Wisent Inc., Canada) and 1% penicillin-streptomycin (Wisent Inc., Canada). THP-1 cells were cultured in complete RPMI 1640 (Wisent Inc., Canada) containing 10% FBS and 1% penicillin-streptomycin. MV-4-11 cells were cultured in complete IMDM (Wisent Inc., Canada) containing 10% FBS and 1% penicillin-streptomycin. All cells were incubated at 37°C in a 5% CO_2 humidified incubator (Thermo Fisher Scientific, USA).

Primary AML Cells

Primary AML cells were obtained from bone marrow collected from patients at diagnosis. Total bone marrow cells were processed immediately and purified by density gradient centrifugation using Ficoll. The mononuclear cell populations were magnetically labeled with CD34 microbeads according to the manufacturer’s instructions (Miltenyi Biotec). $CD34^+$ cells were isolated by immunomagnetic

separation using LS columns and MidiMACS (Miltenyi Biotec), following the manufacturer's protocol. Then the cells were freshly used for experiments or cryopreserved for storage. Sample collection and use were conducted in accordance with the ethical guidelines and protocol approved by the Ethics Committee of the First Affiliated Hospital of Wenzhou Medical University.

Fibrinogen Deficient Mice and AML Mouse Model

All animal experiments were approved by Animal Care and Use Committee of the First Affiliated Hospital of Wenzhou Medical University (Approval file number "WYYY AEC-2024-234"). Fibrinogen deficient ($Fg^{-/-}$) mice have been described previously.[14] To build C1498-GFP AML mouse model, six-week-old C57BL/6 mice (22-24 g) (SLAC ANIMAL, Shanghai, China) were irradiated with 250 cGy X-ray, and were intravenously injected with 1×10^6 C1498-GFP cells suspended in 200 μL phosphate-buffered saline (PBS) per mouse 6 hours (hrs) post irradiation. The bodyweight of mice was monitored every day. Mice used for survival analysis were euthanized when showing visible signs of poor health or physical abnormalities. Mice used for Hematoxylin and Eosin (H&E) Staining and Flow Cytometry analysis were euthanized at day 21, and their liver, spleen, bone marrow (BM) and peripheral blood (PB) were collected for analysis.

Cell Viability Assay

Cell viability was assessed using the Cell Counting Kit-8 (CCK-8, Dojindo, Japan) following the manufacturer's protocol. Briefly, cells were seeded in 96-well plates at a density of 1×10^5 cells per well. After treatment with different concentrations of fibrinogen for 72 hrs, 10 μL of CCK-8 reagent was added to each well and incubated for 3 hrs at 37°C. The absorbance was measured at 450 nm using a microplate reader.

Cell Migration Assay

Cell migration was assessed using transwell assays with 24-well transwell cell culture inserts containing 8 μm pores (Corning, USA). Matrigel was added to the inserts and allowed to solidify for 4 hrs before cell seeding. Cells were plated at a density of 1×10^6 cells/mL in the upper chamber, with 3 g/L fibrinogen included in both the upper and lower chamber media. After 24 hrs, non-migrated cells were gently removed from the upper side of the insert. Cells that had migrated to the bottom of the inserts were collected and counted using 0.4% Trypan Blue (Invitrogen, USA) exclusion assays in triplicate.

Western Blot (WB) Analysis

Total protein was extracted from cells using RIPA lysis buffer (P0013B, Beyotime, China). Protein concentration was determined using the Bicinchoninic acid (BCA) assay (P0010, Beyotime, China). Equal amounts of protein were separated by SDS-PAGE (PG112, Epizyme Biotech, China) and transferred onto PVDF membranes (IPVH00005, Merck, Germany). Membranes were incubated with primary antibodies

against GRP153 (ER63580, HUABIO, China), AKT (EPR16798, Abcam, UK), phospho-AKT1/2/3 (pAKT1/2/3, EPR18853, Abcam, UK), phospho-NDRG1 (pNDRG1, 5482, Cell Signaling Technology, USA), phospho-FOXO1a/3a (pFOXO1a/3a, 9464, Cell Signaling Technology, USA), NDRG1(RM8326, Biodragon, China), FOXO1a/3a (PTM-6083, PTM Bio, China),β-actin (AF003, Beyotime, China) followed by Goat anti-Mouse IgG (H + L) secondary antibody (A0216, Beyotime, China) or Goat anti-Rabbit IgG (H + L) secondary antibody (A0208, Beyotime, China). All primary antibodies were used at a dilution of 1:1000, and secondary antibodies were used at a dilution of 1:2000. Protein bands were visualized using an enhanced chemiluminescence (ECL) detection system (180-501, Tanon, China).

Immunofluorescence Staining

Cells were fixed using 4% paraformaldehyde, permeabilized with 0.2% Triton X-100, and blocked with 5% bovine serum albumin (BSA) before incubation with primary antibodies against pAKT1/2/3 (EPR18853, Abcam, UK). After three washes with PBS, cells were incubated with Cy3-conjugated Affinipure Goat Anti-Rabbit IgG (H + L) secondary antibody (SA00009-2, Proteintech, USA). Nuclei were counterstained with DAPI (Beyotime, China). Slides were sealed with Antifade Mounting Medium (Beyotime, China). Fluorescence images were acquired using a confocal microscope (FV3000, Olympus, Japan) with water as the imaging medium and the imaging

software CellSens Standard (Olympus, Japan). For the analysis, the images were processed using Image J software (National Institutes of Health, USA).

RNA-seq Analysis

Total RNA was extracted from cells using Trizol (Invitrogen, USA). The RNA integrity was assessed by electrophoresis and Agilent 2100 Bioanalyzer (Agilent Technologies, Inc., USA). Paired-end sequencing was performed by Personalbio on Illumina HiSeq. Data QC was performed using Fast QC. Mapping was performed using HISAT2. For miRNA-seq, clean reads were annotated against the miRBase database to identify known miRNAs. Differential gene expression analysis was performed using DESeq.

Quantitative Real-time PCR (RT-qPCR) Analysis

Total RNA was extracted from cells using MiniBEST Universal RNA Extraction Kit (TAKARA, Japan). RNA was reverse-transcribed into cDNA using PrimeScript™ RT Master Mix (Perfect Real Time) (TAKARA, Japan). RT-qPCR was performed using 2×TSINGKE® Master qPCR Mix (SYBR Green I) (Tsingke Biotech, China) on CFX96 Touch Real-Time PCR Detection System (Biorad, USA). Expression levels were normalized to ACTB and analyzed using the $2^{-\Delta\Delta CT}$ method.

miRNA expression was quantified by stem-loop reverse transcription quantitative PCR (RT-qPCR). Total RNA was reverse-transcribed into cDNA using PrimeScript™ RT Master Mix (Perfect Real Time) (TAKARA, Japan) with miRNA-specific stem-

loop RT primers, according to the manufacturer's instructions. RT-qPCR was then performed using miRNA-specific forward primers and a universal reverse primer by 2×TSINGKE® Master qPCR Mix (SYBR Green I) (Tsingke Biotech, China) on CFX96 Touch Real-Time PCR Detection System (Biorad, USA). Expression levels were normalized to U6 and analyzed using the $2^{-\Delta\Delta CT}$ method.

Primer sequences are listed below (5'→3'):

GPR153-F: GGTCTTCGTGTCCACCTTCTAC

GPR153-R: GCCTGCTTCTTGGCATTGCTCA

Rictor-F: CAGTGTGAGGTCCTTTCCATCC

Rictor-R: GCCATAGATGCTTGCGACTGTG

ACTB-F: CACCATTGGCAATGAGCGGTTC

ACTB-R: AGGTCTTTGCGGATGTCCACGT

miR-486-5p-F: CGCGTCCTGTACTGAGCTGC

miR-122-5p-F: CGCGTGGAGTGTGACAATGG

miR-7-5p-F: CGCGTGGAAGACTAGTGATTTT

miRNA-R: AGTGCAGGGTCCGAGGTATT

U6-F: CTCGCTTCGGCAGCACAT

U6-R: TTTGCGTGTCATCCTTGCG

White Blood Cells (WBC) Count

PB were collected from the retro-orbital sinus after anesthetized mice. WBC counts were measured using hematology analyzer (Mindray, China).

Dual-luciferase reporter assay

The 3' untranslated region (3'UTR) of GPR153 were cloned into the psiCHECK vector containing the firefly and renilla luciferase gene. The 3'UTR was connected at the tail of the renilla luciferase gene. HEK-293 cells transfected with GPR153 3'UTR psiCHECK plasmid were then transfected with miR-486-5p mimics/inhibitors and Negative control (NC) mimics for 48 hrs. The fluorescence intensity of firefly and renilla luciferase were detected with Dual-Luciferase Reporter Assay System (E1910, Promega, USA) and microplate reader. miR-486-5p mimics and inhibitors were designed and synthesized by Tsingke Biotech Co., Ltd., China.

Sequence of miR-486-5p mimics: CUCGGGGCAGCUCAGUACAGGA

Sequence of miR-486-5p inhibitors: sense: UCCUGUACUGAGCUGCCCCGAG

antisense: CGGGGCAGCUCAGUACAGGAUU

Flow Cytometry

Single-cell suspensions were prepared from the BM, PB, liver and spleen of fibrinogen knockout and WT mice using ACK lysing buffer (Solarbio, China). Flow cytometry were performed on Gallios Flow Cytometer (Beckman Coulter, USA) and data were analyzed using FlowJo 10 (FlowJo, LLC, USA).

Hematoxylin and Eosin (H&E) Staining

The tissue sections from mice model were stained with H&E according to standard protocols. Images were captured using the light microscope.

GPR153 Overexpression

To overexpress GPR153, its coding sequence from NCBI were cloned into a vector plasmid (pAAV-CMV*p-GPR153*) using the endotoxin-free Maxi Prep Kit (Qiagen, Germany). The resulting plasmid (1 μg) was transfected into 1×10^6 THP-1 cells using 4D Nucleofector System (Core + X Unit, LONZA, Switzerland) and SG Cell Line 4D Nucleofector ™ X Kit (LONZA, Switzerland). Electroporation was conducted following the standard protocol for THP-1 cells, using program FF-100, with the cells suspended in the appropriate electroporation solution. After electroporation, the cells were transferred back into the culture medium and incubated for an additional 48 hrs. Transfection efficiency was subsequently evaluated using RT-qPCR and WB to confirm the overexpression of GPR153.

Knockdown of GPR153

Small interfering RNA (siRNA) targeting GPR153 (siGPR153) was designed and synthesized by Tsingke Biotech Co., Ltd., China. A non-targeting siRNA with a scrambled sequence was used as a negative control. THP-1 cells were transfected with siRNAs using the RNA transfection reagent Entranster™-R4000 (Engreen, New Zealand) according to the manufacturer's instructions. After 3 days of transfection, knockdown efficiency was evaluated by RT-qPCR and WB analysis.

Sequence of siGPR153: CCACCCACAUGCUAAAUGUTT

Statistical Analysis

Survival analysis was performed using GEPIA2 (http://gepia2.cancer-pku.cn/#survival) on the TCGA-LAML cohort; median expression was used as the cutoff, and the final sample size (n=106) reflects cases with available expression and survival data in GEPIA2. Statistical analysis was performed using Prism 9 (GraphPad Software, USA). Data are presented as mean ± standard deviation (SD). T-tests were used for comparing the means of two groups. One way ANOVA followed by Tukey's test were used for comparing the means of three or more groups. Non-parametric tests were used for non-normally distributed data. Differences were considered significant at $p< 0.05$.

Results

Fg promotes AML cell proliferation and migration *via* AKT pathway

We first treated THP-1 cells, a monocyte-derived cell line isolated from the PB of an AML patient, with various concentrations of Fg (0, 1, 2, 3, 4, 5 g/L) for 48 hrs and assessed cell proliferation using CCK-8 assays. The results demonstrated that Fg significantly enhanced THP-1 cell proliferation at all tested concentrations (Figure 1A). Given that Fg circulates in the bloodstream at physiological concentrations of 2–

4 g/L, we selected 3 g/L for further experiments with various AML cell lines, including THP-1, C1498, and MV4-11. Mock-treated cells and those treated with human serum albumin (HSA) served as appropriate controls. Fg-treated cells exhibited significantly faster growth compared to the control groups (Figure 1B and Supplementary Figure 1A). The effect of Fg on AML cell migration was evaluated using transwell migration assays with THP-1 cells. The results revealed that significantly more THP-1 cells migrated in the presence of Fg compared to the control group (Figure 1C).

To determine how AML cells interact with Fg, we next investigated the involvement of integrin receptors previously reported to bind Fg.[15] AML cells were pre-incubated with a blocking antibody against CD11b (integrin αMβ2) prior to Fg treatment. Under these conditions, the Fg-induced proliferative effect was completely abolished. In contrast, pre-treatment with an RGD peptide, which blocks RGD-dependent integrins including αvβ3, did not affect the ability of Fg to promote AML cell proliferation in both THP-1 and C1498 cells (Figure 1D an Supplementary Figure 1B). These results indicate that Fg promotes AML cell proliferation predominantly through integrin αMβ2, rather than αvβ3.

To investigate the molecular mechanisms underlying the effects of Fg, we focused on the AKT/mTOR signaling pathway, which is pivotal in leukemogenesis and regulates AML cell growth and survival.[16-18] WB analysis revealed significant increases in the levels of pAKT, pFOXO1/3a, and pNDRG1 following Fg treatment (Figure 1E), indicating activation of the AKT pathway. Additionally, immunofluorescence analysis

confirmed a marked increase in AKT phosphorylation in AML cells treated with Fg (Figure 1F). Taken together, these results demonstrate that Fg promotes the proliferation and migration of AML cells and was associated with the activation of the AKT signaling pathway.

Fg down-regulates the orphan receptor GPR153 in AML cells

To further elucidate the mechanism by which Fg promotes AML progression, RNA-seq was performed on THP-1 cells treated with 3 g/L Fg for 72 hrs. Among the differentially expressed genes identified by RNA-seq, a subset of GPCR genes was significantly altered following Fg treatment (Figure 2A). Notably, the orphan receptor GPR153 was found to be highly down-regulated (Figure 2B). These RNA-seq findings were corroborated by RT-qPCR in THP-1 and C1498 cells, which both demonstrated a significant reduction in GPR153 expression at mRNA level following Fg treatment (Figure 2C). The reduction of GPR153 at protein level was further validated by WB analysis in THP-1 cells (Figure 2D). Recent studies have indicated that GPR153 is overexpressed in AML cases with the t(8;21) translocation, which is associated with a favorable prognosis.[19] In line with this, data from The Cancer Genome Atlas (TCGA) were analyzed, revealing that higher GPR153 expression correlated with favorable survival outcomes in AML patients (Figure 2E). These findings suggest that GPR153 functions as a tumor suppressor in AML progression, and that Fg may promote AML progression by downregulating GPR153, thereby

attenuating its tumor-suppressive effects.

The orphan receptor GPR153 is a key mediator of Fg-induced AML progression

To further elucidate the role of the orphan receptor GPR153 in the regulatory effects of Fg on AML progression, we knocked down GPR153 in THP-1 cells using siRNA (Figure 3A). CCK-8 and transwell assays revealed that GPR153 silencing alone significantly enhanced the proliferation and migration of THP-1 cells (Figure 3B, C). Notably, Fg treatment failed to further increase the proliferation or migration of GPR153-deficient AML cells, indicating that the effects of Fg on AML cell are largely dependent on GPR153. WB analysis showed that pAKT levels were significantly elevated following GPR153 knockdown while total AKT expression remained unchanged, indicating the activation of AKT/mTOR signaling pathway (Figure 3D). To further validate these findings, GPR153 was overexpressed in THP-1 cells, which was validated by RT-qPCR (Figure 3E) and WB analysis (Figure 3F). The overexpression of GPR153 significantly reduced the proliferation of THP-1 cells (Figure 3G).And showed resistance to Fg-induced migration (Figure 3H). In addition, as shown in Figure 3I, pAKT levels were markedly reduced in the Fg-treated OE GPR153 group compared with the Fg-treated control group. These data highlights the pivotal role of GPR153 in Fg-induced AML progression and its regulation of the AKT/mTOR signaling pathway.

GPR153 is regulated by miR-486-5p in AML cells

To investigate how GPR153 expression is regulated, we utilized TargetScan and miRDB, to predict potential miRNAs that target the 3' UTR of GPR153. This analysis identified 158 candidate miRNAs (Supplementary Figure 2A). Among these candidates, RNA-seq analysis of Fg-treated THP-1 cells revealed significant changes in only three miRNAs: the up regulation of miR-486-5p and miR-122-5p and the downregulation of miR-7-5p. Further RT-qPCR confirmed that miR-486-5p was significantly upregulated in Fg-treated THP-1 cells (Figure 4A). Notably, miR-486-5p has previously been identified as an erythroid oncomiR in Down syndrome-associated myeloid leukemia and has been linked to AML progression and clinical outcomes.[20, 21] In line with this, data from TCGA-LAML cohort revealed that lower miR-486-5p expression correlated with favorable survival outcomes in AML patients (Figure 4B). To confirm whether GPR153 is a direct target of miR-486-5p, we performed dual-luciferase reporter assays in HEK293 cells. The wild-type or mutant 3'UTR of GPR153 was cloned into the psiCHECK plasmid (Supplementary Figure 2B), which was then co-transfected with miR-486-5p mimics or a negative control. The transfection efficiency of miR-486-5p mimics and inhibitor was confirmed by RT-qPCR (Figure 4C). As shown in Figure 4D, miR-486-5p mimics significantly reduced the relative luciferase expression, whereas this suppression was abolished when the seed region was mutated, confirming a direct interaction between miR-486-5p and the 3'UTR of GPR153. Moreover, examined by WB analysis, overexpression of miR-486-5p markedly reduced GPR153 protein levels (Figure 4E). To further validate this

regulation, we transfected THP-1 cells with a miR-486-5p inhibitor prior to Fg treatment, which effectively rescued the Fg-induced downregulation of GPR153 (Figure 4F).

Fg deficiency inhibits AML progression by down-regulating the AKT pathway *in vivo*

To validate our findings *in vivo*, we established AML mouse models with $Fg^{-/-}$ and wild-type (WT) backgrounds. GFP+ C1498 cells were engineered and validated (Supplementary Figure 3), then injected into sublethally irradiated $Fg^{-/-}$ and WT mice *via* tail vein (Figure 5A). Kaplan-Meier survival analysis revealed that $Fg^{-/-}$ mice had significantly longer overall survival compared to WT mice [median survival: 30 days (range 27–35) vs. 26 days (range 22–28); P = 0.0163] (Figure 5B). At 21 days post-injection, PB examination showed lower WBC counts and reduced percentages of GFP+ C1498 cells in the $Fg^{-/-}$ mice compared to the WT mice (Figure 5C, D). Additionally, the size and weight of both liver and spleen were lower in $Fg^{-/-}$ mice than those of WT mice (Figure 6A, B). Flow cytometry further revealed significantly lower percentage of GFP+ C1498 cells in the liver, spleen, and BM of $Fg^{-/-}$ mice, indicating the reduction of leukemia cell infiltration (Figure 6C, Supplementary Figure 4). These findings were further confirmed by H&E staining (Figure 6D).

Further analysis of GFP+ C1498 cells isolated from PB revealed a significant reduction in Rictor mRNA levels (Figure 7A)， and pAKT protein level in $Fg^{-/-}$

mice compared to the WT mice, indicating Fg activated the mTORC2/AKT pathway (Figure 7B). Furthermore，immunofluorescence analysis of GFP□ C1498 cells isolated from PB confirmed the reduction of pAKT in Fg□/□ mice (Figure 7C), validating that the AKT pathway was inhibited in the absence of Fg. Moreover, WB analysis also verified the down-regulation of Fg on GPR153 *in vivo* (Figure 7B). These *in vivo* results align with our *in vitro* findings, providing strong evidence that Fg promotes AML progression through the activation of the mTORC2/AKT pathway.

Fg promotes migration of primary AML cells through miR-486/GPR153 axis

To assess whether Fg promotes patient-derived primary AML cells via the GPR153/miR-486 axis, we examined cells from 4 newly diagnosed AML patients . (Supplementary Table 1). Primary AML cells were treated with 3 g/L Fg for 48 h, qRT-PCR revealed that miR-486 was markedly upregulated in all of the 4 patients (Figure 8A). GPR153 mRNA was reduced in Patients 2, 3 and 4, but was not apparent in Patient 1 (Figure 8B). Extramedullary infiltration was observed in Patient 2 and Patient 3, that was hepatomegaly, splenomegaly and lymphadenopathy respectively (Supplementary Table 1). To test whether Fg influences this migratory behavior, we performed transwell assays. The results showed that Fg increased migration of primary cells from Patients 2, 3 and 4 but did not exert a positive effect on primary cells from Patients 1 (Figure 8C), which was in line with the pattern of GPR153

expression. Immunofluorescence for pAKT also paralleled the molecular experiment results. Primary cells from Patients 2, 3 and 4 displayed clear increases in pAKT after Fg treatment, whereas Patients 1 showed little change (Figure 8D&E). Together, these data indicate that Fg can downregulate GPR153 and upregulate miR-486 in primary AML cells, leading to AKT activation and enhanced migration.

Discussion

Researches on Fg and cancer are predominantly limited to clinical data analysis, revealing that high Fg levels are associated with poor survival in multiple cancers, including colorectal cancer (CRC), non-small cell lung cancer (NSCLC), and pancreatic ductal adenocarcinoma (PDAC).[22, 23] Recent studies generated Fg knockout mice provided a deeper understanding on the role of Fg in tumorigenesis and tumor development. Fg is aberrantly deposited in the tumor microenvironment, where it can stimulate immune cells to secrete pro-inflammatory cytokines, contributing to the tumor progression. Fg also facilitates tumor cell dissemination by linking the integrin αvβ3 on tumor cells with αIIbβ3 on platelets through its RGD sequence.[24] However, whether Fg exerts a similar pro-tumor effect in hematologic malignancies, particularly AML, has remained unclear.

In this study, we developed a Fg deficient AML mouse model and confirmed that Fg promotes AML cell proliferation and migration, thereby accelerating disease progression. We further demonstrated that Fg upregulates miR-486-5p both in AML

cell lines and primary AML cells from 4 newly diagnosed AML patients. It was reported that in solid tumors such as lung, liver, and breast cancer, the miR-486-5p is downregulated and acts as a tumor suppressor, inhibiting growth and metastasis.[25] In contrast, in AML and chronic myeloid leukemia (CML), miR-486-5p is upregulated and contributes to disease pathogenesis by modulating the JAK-STAT signaling pathway.[21, 26] These findings support the potential oncogenic role of miR-486-5p in hematological malignancies. Although miR-486-5p has been reported to modulate JAK/STAT signalling, we did not observe consistent regulation of representative STAT downstream target genes (MCL1, BCL2, BCL-xL) following Fg treatment across AML cell lines (Supplementary Figure 5). Nevertheless, a context-dependent contribution of JAK/STAT signalling cannot be excluded and warrants further study.

In 2016, Maiga A reported that GPR153 was highly expressed in AML patients with the t(8;21) genetic subgroup, a feature linked to better prognosis.[19] Moreover, data from TCGA confirmed that high GPR153 expression correlated with improved survival in AML patients, highlighting GPR153 act as a tumor suppressor in AML progression. Consistently, Our study showed that AML cells from Fg-deficient mice exhibited elevated GPR153 levels, which were associated with better outcomes. Furthermore, overexpressing GPR153 inhibited the Fg-induced proliferation and migration of AML cells. Dual luciferase assay was performed to confirm the direct regulatory relationship between miR-486-5p and GPR153. Hence, these findings confirmed that miR-486-5p promoted AML progression by targeting and suppressing GPR153.

The AKT/mTOR pathway plays a critical role in AML development, being activated in approximately 60% of patients and regulating AML cell growth and survival. mTOR functions as a protein kinase in two complexes: mTORC1 (comprising mTOR, Raptor, Pras40, mLST8, and Deptor, with S6K1 and 4E-BP as downstream targets) and mTORC2 (including Rictor, mSIN1, Protor-1, mLST8, and Deptor, targeting AKT). [27]

In this study, Fg treatment consistently increased phosphorylation of AKT at Ser473, which is commonly associated with mTORC2 activity. Based on this observation, together with the increased expression of Rictor after Fg treatment, we focused on the potential involvement of mTORC2 signaling pathway. Rictor is a critical structural and functional component of mTORC2 and is required for efficient AKT Ser473 phosphorylation, thereby supporting malignant cell growth, survival, and migration. Our findings revealed that Fg upregulates Rictor expression and enhances AKT phosphorylation. Notably, GPR153 knockdown activated the mTORC2/AKT pathway, whereas its overexpression attenuated the Fg-induced proliferation and migration of AML cells. Thus, Fg exacerbates AML progression by upregulating miR-486-5p, which targets GPR153, ultimately activating the mTORC2/AKT pathway to drive AML cell growth and migration. However, further studies will be required to distinguish the contributions of mTORC1 and mTORC2 in this process. Overall, this study provides mechanistic insights into Fg’s role in AML, particularly its interaction with circulating AML cells.

Consistent with the multifaceted roles of fibrinogen in cancer biology, prior studies have shown that Fg can regulate tumor progression through distinct molecular mechanisms depending on tumor type and microenvironmental context. In breast cancer, Fg within the extracellular matrix modulates tumor cell proliferation and dormancy through mechanical stimuli. In esophageal squamous cell carcinoma (ESCC), Fg enhances cell motility by inducing EMT *via* the p-AKT/p-mTOR pathway.[28] In colon cancer, Fg promotes proliferation and prevents tumor cell senescence by activating FAK and inhibiting p53, subsequently affecting downstream targets such as 14-3-3σ and p21. These observations highlight that Fg does not engage a uniform oncogenic signaling program across malignancies. Rather, its downstream effects appear to be highly context-dependent. Our study detailed the regulatory mechanisms by which Fg promotes AML progression in both animal models and primary human cells. Using primary blasts from 4 newly diagnosed AML patients, we found that Fg enhanced migration, upregulated miR-486 expression, and activated mTORC2/AKT pathway in samples from patients 2, 3 and 4, concordant with our hypothesis. However, primary AML cells from patient 1 did not exhibit Fg-induced migration, nor did Fg decreased GPR153 level or AKT phosphorylation in that sample. We speculate that the different response of patient 1 reflects intrinsic heterogeneity among AML cases. As shown in Table 1, patient 1 was classified as AML with maturation, whereas the human AML cell lines used in our *in vitro* work THP-1 were more consistent with acute monoblastic/monocytic leukemia. Moreover, unlike patients 2–4 whose peripheral WBC counts were elevated, patient 1 had a normal

WBC count and substantially lower blast percentages in both peripheral blood and bone marrow. These clinical differences may underlie the divergent experimental results. Future studies should include a larger, subtype-stratified cohort to delineate how Fg regulates AML progression across distinct AML subtypes.

Our findings, showing that Fg knockout significantly reduced tumor burden in AML mouse model, suggest the potential of Fg as a therapeutic molecular target. Given that fibrinogen is synthesized in the liver, and that small RNA drug delivery technologies targeting the liver have been well-established, the therapeutic potential of Fg knockdown using recombinant adeno-associated virus (rAAV) vectors or lipid nanoparticles (LNPs) on AML progression is worth further investigation in future studies. A limitation of the current study is that fibrinogen supplementation in $Fg^{-/-}$ mice was not feasible due to coagulation defects and the requirement for repeated dosing. Future studies using alternative delivery strategies such as rAAV vectors, will be required to address this.

In conclusion, our study revealed the molecular mechanism of Fg accelerates AML progression, that induces miR-486-5p expression and targets the orphan receptor GPR153. This leads to the activation of mTORC2/AKT pathway, ultimately driving AML cell proliferation and migration. Our findings also implied the value of fibrinogen as a therapeutic molecular target.

References

1. Petersen MA, Ryu JK, Akassoglou K. Fibrinogen in neurological diseases: mechanisms, imaging and therapeutics. Nat Rev Neurosci. 2018;19(5):283-301.
2. Sharma BK, Mureb D, Murab S, et al. Fibrinogen activates focal adhesion kinase (FAK) promoting colorectal adenocarcinoma growth. J Thromb Haemost. 2021;19(10):2480-2494.
3. Zheng S, Shen J, Jiao Y, et al. Platelets and fibrinogen facilitate each other in protecting tumor cells from natural killer cytotoxicity. Cancer Sci. 2009;100(5):859-865.
4. Sahni A, Arévalo MT, Sahni SK, Simpson-Haidaris PJ. The VE-cadherin binding domain of fibrinogen induces endothelial barrier permeability and enhances transendothelial migration of malignant breast epitelial cells. Int J Cancer. 2009;125(3):577-584.
5. Miller BE, Tal-Singer R, Rennard SI, et al. Plasma fibrinogen qualification as a drug development tool in chronic obstructive pulmonary disease. Perspective of the chronic obstructive pulmonary disease biomarker qualification consortium. Am J Respir Crit Care Med. 2016;193(6):607-613.
6. Dai K, Zhang Q, Li Y, Wu L, Zhang S, Yu K. Plasma fibrinogen levels correlate with prognosis and treatment outcome in patients with non-M3 acute myeloid leukemia. Leuk Lymphoma. 2019;60(6):1503-1511.
7. Berger MD, Heini AD, Seipel K, Mueller B, Angelillo-Scherrer A, Pabst T. Increased fibrinogen levels at diagnosis are associated with adverse outcome in patients with acute myeloid leukemia. Hematol Oncol. 2017;35(4):789-796.
8. Zhang Z, Zhang R, Qi J, et al. The prognostic value of plasma fibrinogen level in patients with acute myeloid leukemia: a systematic review and meta-analysis. Leuk Lymphoma. 2020;61(11):2682-2691.
9. Akimoto M, Sakurai A, Nishiyama-Fujita Y, Ito C, Aisa Y, Nakazato T. The prognostic value of the Fibrinogen-Albumin Ratio Index in patients with myelodysplastic syndrome and acute myeloid leukemia with myelodysplasia-related changes treated with azacitidine. Ann Hematol. 2021;100(4):953-957.
10. Nepstad I, Hatfield KJ, Grønningsæter IS, Reikvam H. The PI3K-Akt-mTOR signaling pathway in human acute myeloid leukemia (AML) cells. Int J Mol Sci. 2020;21(8):2907.
11. Zeng Z, Shi YX, Tsao T, et al. Targeting of mTORC1/2 by the mTOR kinase inhibitor PP242 induces apoptosis in AML cells under conditions mimicking the bone marrow microenvironment. Blood. 2012;120(13):2679-2689.
12. Calebiro D, Koszegi Z, Lanoiselée Y, Miljus T, O'Brien S. G protein-coupled receptor-G protein interactions: a single-molecule perspective. Physiol Rev. 2021;101(3):857-906.
13. O'Hayre M, Degese MS, Gutkind JS. Novel insights into G protein and G protein-coupled receptor signaling in cancer. Curr Opin Cell Biol. 2014;27:126-135.
14. Suh TT, Holmbäck K, Jensen NJ, et al. Resolution of spontaneous bleeding events but failure of pregnancy in fibrinogen-deficient mice. Genes Dev. 1995;9(16):2020-2033.
15. Yokoyama K, Zhang X-P, Medved L, Takada Y. Specific binding of integrin αvβ3 to the fibrinogen γ and αE chain C-terminal domains. Biochemistry. 1999;38(18):5872-5877.
16. Bertacchini J, Heidari N, Mediani L, et al. Targeting PI3K/AKT/mTOR network for treatment of leukemia. Cell Mol Life Sci. 2015;72(12):2337-2347.
17. Tamburini J, Elie C, Bardet V, et al. Constitutive phosphoinositide 3-kinase/Akt activation represents a favorable prognostic factor in de novo acute myelogenous leukemia patients. Blood. 2007;110(3):1025-1028.

18. Xu Q, Simpson S-E, Scialla TJ, Bagg A, Carroll M. Survival of acute myeloid leukemia cells requires PI3 kinase activation. Blood. 2003;102(3):972-980.
19. Maiga A, Lemieux S, Pabst C, et al. Transcriptome analysis of G protein-coupled receptors in distinct genetic subgroups of acute myeloid leukemia: identification of potential disease-specific targets. Blood Cancer J. 2016;6(6):e431.
20. Shaham L, Vendramini E, Ge Y, et al. MicroRNA-486-5p is an erythroid oncomiR of the myeloid leukemias of Down syndrome. Blood. 2015;125(8):1292-1301.
21. Sha C, Jia G, Jingjing Z, Yapeng H, Zhi L, Guanghui X. miR-486 is involved in the pathogenesis of acute myeloid leukemia by regulating JAK-STAT signaling. Naunyn Schmiedebergs Arch Pharmacol. 2021;394(1):177-187.
22. Huang W, Wang S, Zhang H, Zhang B, Wang C. Prognostic significance of combined fibrinogen concentration and neutrophil-to-lymphocyte ratio in patients with resectable non-small cell lung cancer. Cancer Biol Med. 2018;15(1):88-96.
23. Chung KH, Lee J-C, Lee J, et al. Serum fibrinogen as a diagnostic and prognostic biomarker for pancreatic ductal adenocarcinoma. Pancreatology. 2020;20(7):1465-1471.
24. Wu X, Yu X, Chen C, et al. Fibrinogen and tumors. Front Oncol. 2024;14:1393599.
25. Ding L, Tian W, Zhang H, et al. MicroRNA-486-5p suppresses lung cancer via downregulating mTOR signaling in vitro and in vivo. Front Oncol. 2021;11:655236.
26. Suchiita A, Guru SA, Yadav P, et al. miR-486-5p: a prognostic biomarker for chronic myeloid leukemia. ACS omega. 2021;6(11):7711-7718.
27. Panwar V, Singh A, Bhatt M, et al. Multifaceted role of mTOR (mammalian target of rapamycin) signaling pathway in human health and disease. Signal Transduct Target Ther. 2023;8(1):375.
28. Zhang F, Wang Y, Sun P, et al. Fibrinogen promotes malignant biological tumor behavior involving epithelial–mesenchymal transition via the p-AKT/p-mTOR pathway in esophageal squamous cell carcinoma. J Cancer Res Clin Oncol. 2017;143(12):2413-2424.

Figure Legend

Figure 1. Fg promotes AML cell proliferation and migration *via* AKT pathway.

(A) Fg promoted the proliferation of THP-1 cells at varying concentrations of 1, 2, 3, 4, and 5 g/L, as evaluated by CCK-8 assay (***p<0.001). (B) 3g/L Fg promoted the proliferation of THP-1 cells, as evaluated by CCK-8 assay (***p<0.001; ns, not significant). (C) 3g/L Fg promoted the migration of THP-1 cells determined by transwell assay, expressed as cells per 10^4/mL (***p<0.001). (D) THP-1 cells were pre-incubated with a blocking antibody against CD11b (integrin αMβ2) or with an RGD peptide prior to 3g/L Fg treatment. Cell proliferation was assessed at 48 hrs. (E) WB analysis of THP-1 and C1498 cells treated with 3g/L Fg revealed elevated levels of pAKT, pNDRG1, and pFOXO1a/3a. (F) Elevated pAKT levels in Fg-treated THP-1 and C1498 cells were visualized after immunofluorescence staining, confirming the activation of the AKT pathway.

Figure 2. Fg down-regulates the orphan receptor GPR153 in AML cells. THP-1 and C1498 cells were treated with 3 g/L Fg for 72 hrs. (A) Differential gene expression analysis of THP-1 cells revealed the obvious downregulation of the orphan receptor GPR153. (B) A box plot illustrates the decreased level of GPR153 in Fg-treated THP-1 cells (***p < 0.001). (C) Decreased GPR153 expression levels in THP-1 and C1498 cells were further validated by RT-qPCR (***p < 0.001). (D) Decreased GPR153 expression levels in THP-1 cells were confirmed by WB analysis (**p <

0.01). (E) The Kaplan-Meier survival curve demonstrates better overall survival in high GPR153 expression patients (p=0.03).

Figure 3. The orphan receptor GPR153 is a key mediator of Fg-induced AML progression.

(A) The expression level of GPR153 was significantly decreased in THP-1 cells after knockdown using siRNA (***p<0.001). (B) Proliferation of THP-1 cells was enhanced after knockdown the GPR153, as assessed by the CCK-8 assay (*p<0.05, **p<0.01). 3g/L Fg treatment failed to further enhance proliferation in GPR153-knockdown cells. (C) Migration of THP-1 cells was enhanced after knockdown the GPR153, as evaluated by Transwell assay (***p < 0.001). 3g/L Fg treatment failed to further enhance migration in GPR153-knockdown cells. (D) WB analysis confirmed the level of pAKT was elevated in GPR153-knockdown THP-1 cells. (E) GPR153-overexpressing THP-1 cells were generated by electroporation, and the elevated level of GPR153 was confirmed by RT-qPCR (***p<0.001). (F) WB analysis confirmed the overexpression of GPR153 in THP-1 cells following electroporation. (G) GPR153 overexpression impeded the proliferation of THP-1 cells (***p<0.001). (H) GPR153 overexpression impeded the migration of THP-1 cells induced by Fg (*p<0.05). (I) WB analysis showed the level of pAKT was reduced in 3g/L Fg-treated GPR153-knockdown THP-1 cells compared with 3g/L Fg-treated control THP-1 cells.

Figure 4. GPR153 is regulated by miR-486-5p in AML cells.

(A) RT-qPCR validated up-regulation of miR-486-5p in Fg-treated THP-1 cells (****p<0.0001, ND = Not detected). (B) The Kaplan-Meier survival curve on TCGA-LAML cohort demonstrates better overall survival in low miR-486-5p expression patients. (C) Transfection efficiency of miR-486-5p mimics and inhibitor in THP-1 cells was validated by RT-qPCR, showing a marked increase and decline respectively in miR-486-5p expression compared with the negative control. (D) Dual-luciferase reporter assay demonstrated that miR-486-5p significantly reduced the relative luciferase activity of the WT GPR153 3' UTR reporter, whereas mutation of the miR-486-5p seed-binding site abolished this suppressive effect. (E) WB analysis confirmed that transfection with miR-486-5p mimics reduced GPR153 protein levels in THP-1 cells. (F) Inhibition of miR-486-5p rescued the Fg-induced downregulation of GPR153, as determined by RT-qPCR analysis.

Figure 5. Fg promotes AML progression *in vivo*.

(A) Fg homozygous knockout ($Fg^{-/-}$) C57BL/6 mice, paired with WT mice were constructed. The workflow of *in vivo* experiment were illustrated using schematic diagram. (B) Kaplan–Meier survival curve showed prolonged survival in the $Fg^{-/-}$ AML mice group compared to WT AML group (*P=0.0163). (C) AML mice were sacrificed on day 21, and the total number of PB leukocytes was lower in the $Fg^{-/-}$ mice group compared to the WT group (***p<0.001). (D) The percentage of AML

(*GFP*$^{+}$ C1498) cells was significantly reduced in the Fg$^{-/-}$ mice group compared to the WT group (*p<0.05).

Figure 6. Fg promotes AML migration *in vivo*.

(A) Representative images of liver and spleen from Fg$^{-/-}$ and WT AML mice. (B) The spleen and liver weights of AML mice were significantly lower in the Fg$^{-/-}$ group compared to the WT group (*p<0.05). (C) Flow cytometric analysis showed the percentage of *GFP*$^{+}$ C1498 cells in PB, BM, liver, and spleen was significantly lower in the Fg$^{-/-}$ mice group compared to the WT group (*p<0.05, **p<0.01). (D) H&E staining of the liver and spleen demonstrated fewer infiltrations of AML cells in the liver and spleen of sacrificed Fg$^{-/-}$ mice compared to the WT mice.

Figure 7. Fg promotes AML progression *via* AKT pathway *in vivo*.

(A) *GFP*$^{+}$ C1498 cells were sorted from PB of Fg$^{-/-}$ and WT AML mice, with sorted leukocytes from WT healthy mice as controls. RT-qPCR analysis showed elevated Rictor level in WT AML mice, which was significantly reduced in Fg$^{-/-}$ mice (*p<0.05). (B) WB analysis demonstrated the elevated pAKT level in WT AML mice and reduced pAKT level in Fg$^{-/-}$ mice, and GPR153 was reduced in WT AML mice. (C) Immunofluorescence examination visualized the elevated pAKT levels in WT AML mice were eliminated, which were notably diminished in Fg$^{-/-}$ AML mice.

Figure 8. Fg promotes migration of primary AML cells through miR-486/GPR153 axis

Primary AML cells were collected from 4 newly diagnosed patients, and were treated with 3 g/L Fg for 72 hrs. (A) miR-486 and (B) GPR153 expression levels were determined by RT-qPCR. (C) GPR153 expression level were determined by WB. (D) Transwell migration assays of primary AML cells with or without Fg treatment. Fg enhanced migration in Patients 2, 3 and 4, but not in Patients 1. (E) Quantification of pAKT immunofluorescence intensity in primary AML cells of the 4 patients. pAKT levels were increased after Fg treatment in Patients 2, 3, and 4, but not in Patient 1. (F) Representative immunofluorescence images of pAKT in primary AML cells with or without Fg treatment. Scale bar = 100 μm.

Abbreviation

3'UTR: 3' untranslated region

AML: acute myeloid leukemia

BCA: Bicinchoninic acid

BM: bone marrow

BSA: bovine serum albumin

CCK-8: Cell Counting Kit-8

CML: chronic myeloid leukemia

CRC: colorectal cancer

DFS: disease-free survival

ECL: enhanced chemiluminescence

EMT: epithelial-mesenchymal transition

ESCC: esophageal squamous cell carcinoma

FAK: focal adhesion kinase

FARI: fibrinogen-albumin ratio index

Fg: fibrinogen

$Fg^{-/-}$: Fibrinogen deficient

GPCRs: G protein-coupled receptors

HSA: human serum albumin

hrs: hours

H&E: Hematoxylin and Eosin

LNPs: lipid nanoparticles

NK: natural killer

NSCLC: non-small cell lung cancer

OS: overall survival

PB: peripheral blood

PBS: phosphate-buffered saline

PDAC: pancreatic ductal adenocarcinoma

rAAV: recombinant adeno-associated virus

RNA-seq: RNA sequencing

RT-qPCR: quantitative real-time PCR

SD: standard deviation

siRNA: small interfering RNA

WB : Western Blot

WT: wild-type

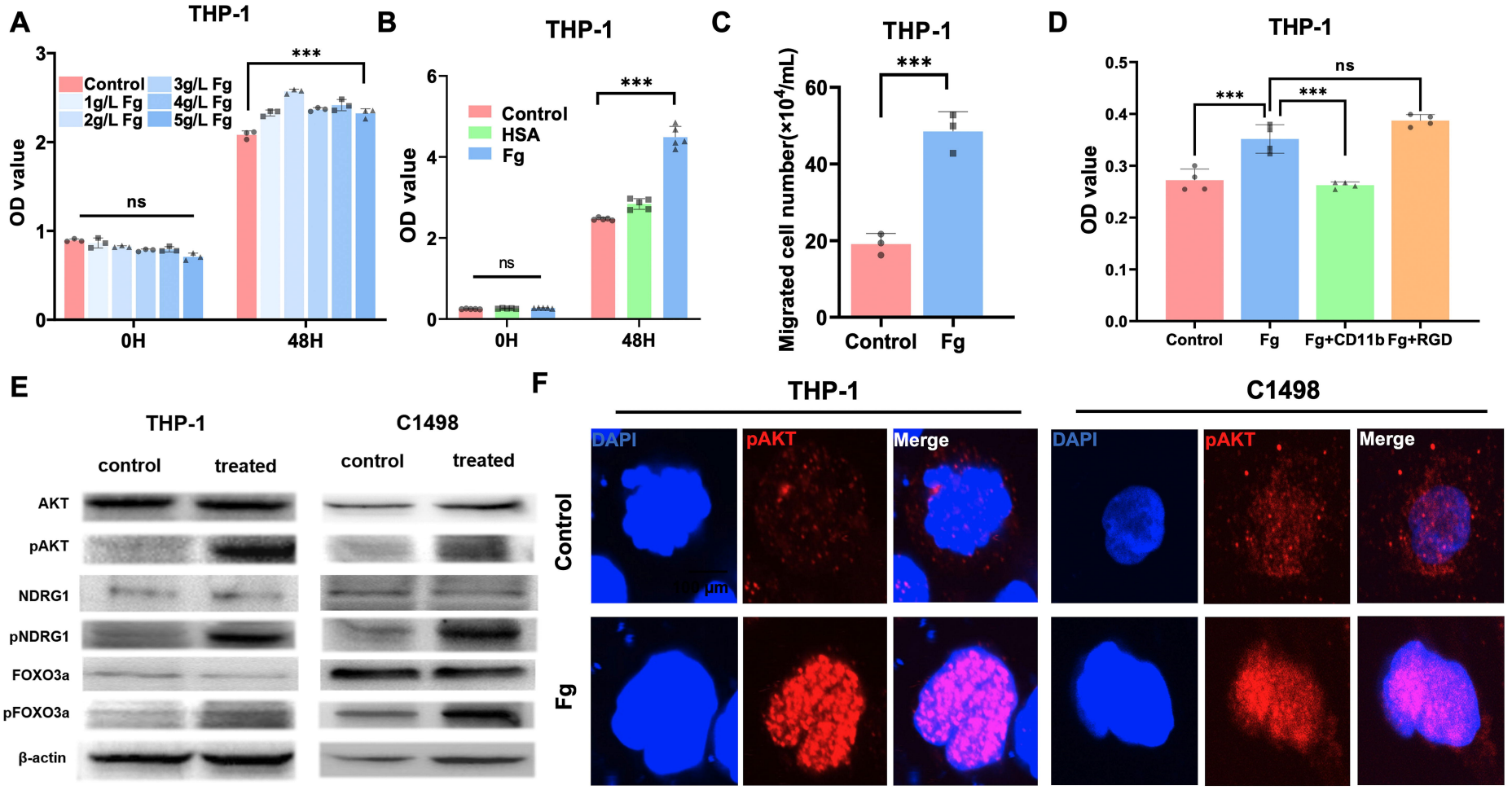
A
THP-1
OD value
Control
1g/L Fg
2g/L Fg
3g/L Fg
4g/L Fg
5g/L Fg
***
ns
0H
48H
B
THP-1
OD value
Control
HSA
Fg
***
ns
0H
48H
C
THP-1
Migrated cell number(×10⁴/mL)
***
Control
Fg
D
THP-1
OD value
***
***
ns
Control
Fg
Fg+CD11b
Fg+RGD
E
THP-1
C1498
control
treated
control
treated
AKT
pAKT
NDRG1
pNDRG1
FOXO3a
pFOXO3a
β-actin
F
THP-1
C1498
DAPI
pAKT
Merge
Control
Fg
100 μm

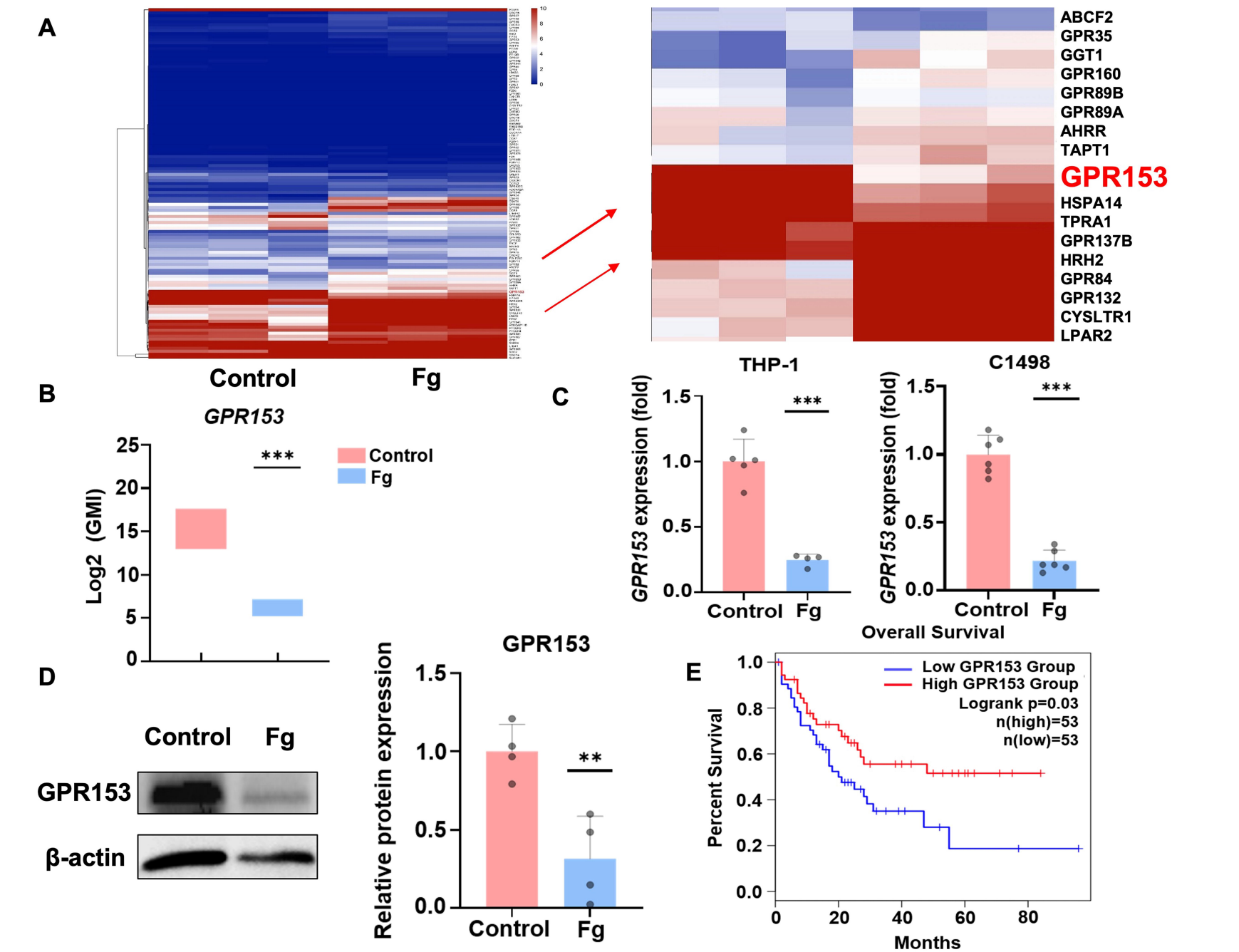
A
Control
Fg
ABCF2
GPR35
GGT1
GPR160
GPR89B
GPR89A
AHRR
TAPT1
GPR153
HSPA14
TPRA1
GPR137B
HRH2
GPR84
GPR132
CYSLTR1
LPAR2
B
GPR153
Log2 (GMI)
***
Control
Fg
C
THP-1
C1498
GPR153 expression (fold)
***
Control
Fg
D
Control
Fg
GPR153
β-actin
GPR153
Relative protein expression
**
E
Overall Survival
Low GPR153 Group
High GPR153 Group
Logrank p=0.03
n(high)=53
n(low)=53
Percent Survival
Months

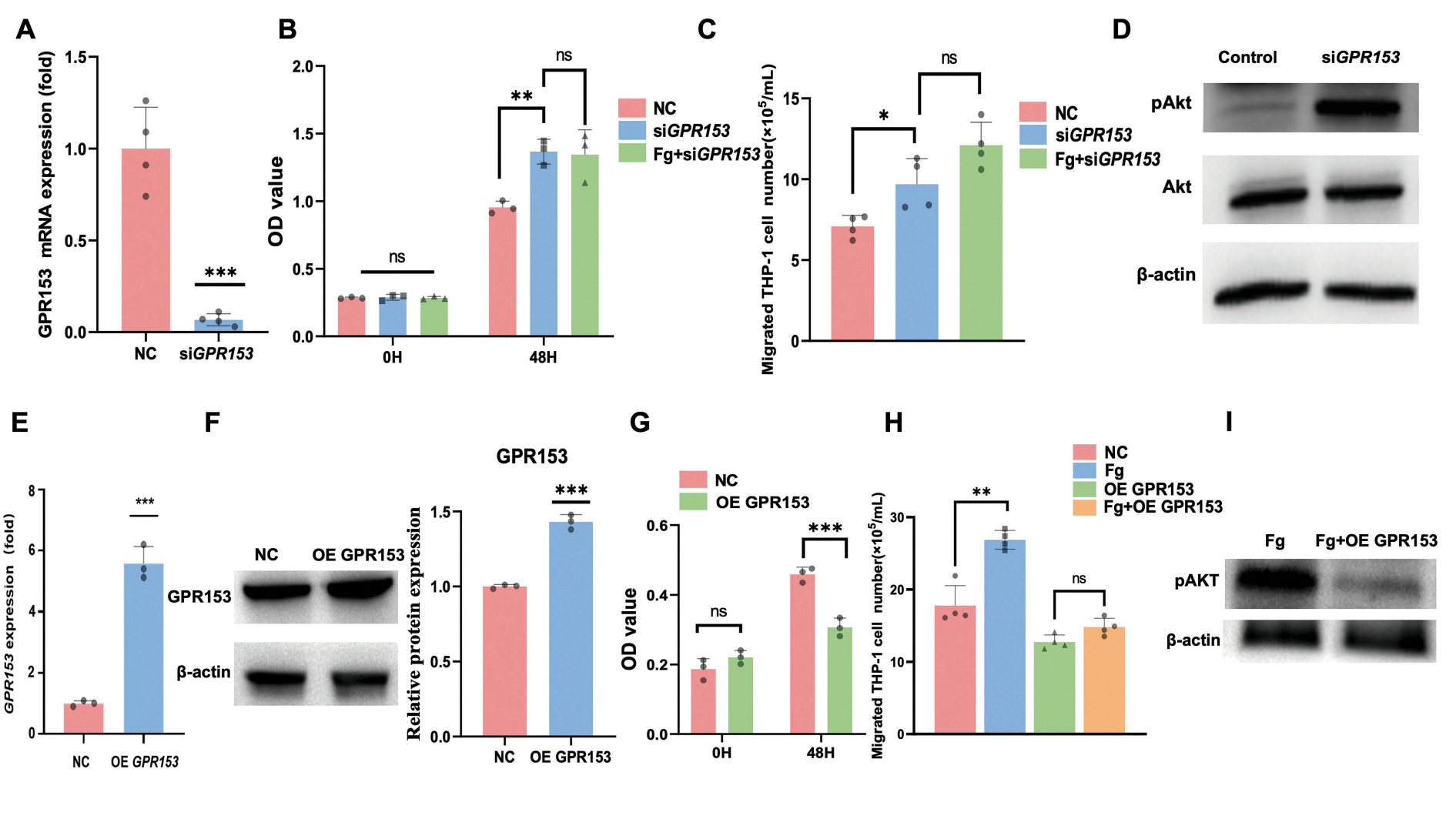
A
GPR153 mRNA expression (fold)
1.5
1.0
0.5
0.0
***
NC
siGPR153
B
OD value
2.0
1.5
1.0
0.5
0.0
ns
**
ns
0H
48H
NC
siGPR153
Fg+siGPR153
C
Migrated THP-1 cell number(×10^5/mL)
15
10
5
0
*
ns
NC
siGPR153
Fg+siGPR153
D
Control
siGPR153
pAkt
Akt
β-actin
E
GPR153 expression (fold)
8
6
4
2
0
***
NC
OE GPR153
F
NC
OE GPR153
GPR153
β-actin
GPR153
Relative protein expression
1.5
1.0
0.5
0.0
***
NC
OE GPR153
G
NC
OE GPR153
OD value
0.6
0.4
0.2
0.0
ns
***
0H
48H
H
NC
Fg
OE GPR153
Fg+OE GPR153
Migrated THP-1 cell number(×10^5/mL)
30
20
10
0
**
ns
I
Fg
Fg+OE GPR153
pAKT
β-actin

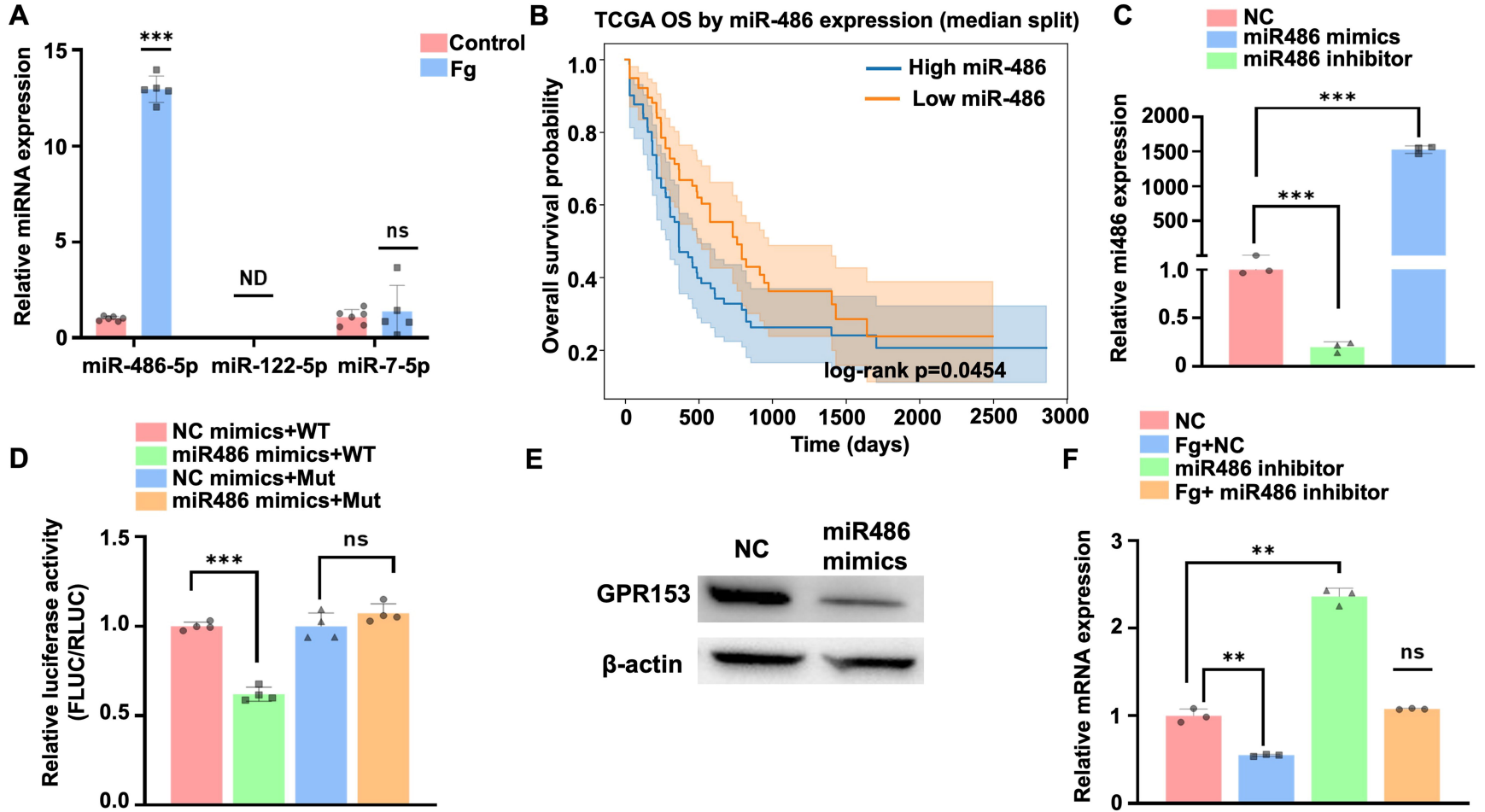
A
Relative miRNA expression
Control
Fg
***
ns
ND
miR-486-5p
miR-122-5p
miR-7-5p
B
TCGA OS by miR-486 expression (median split)
High miR-486
Low miR-486
Overall survival probability
log-rank p=0.0454
Time (days)
C
NC
miR486 mimics
miR486 inhibitor
Relative mi486 expression
D
NC mimics+WT
miR486 mimics+WT
NC mimics+Mut
miR486 mimics+Mut
Relative luciferase activity (FLUC/RLUC)
E
NC
miR486 mimics
GPR153
β-actin
F
NC
Fg+NC
miR486 inhibitor
Fg+ miR486 inhibitor
Relative mRNA expression

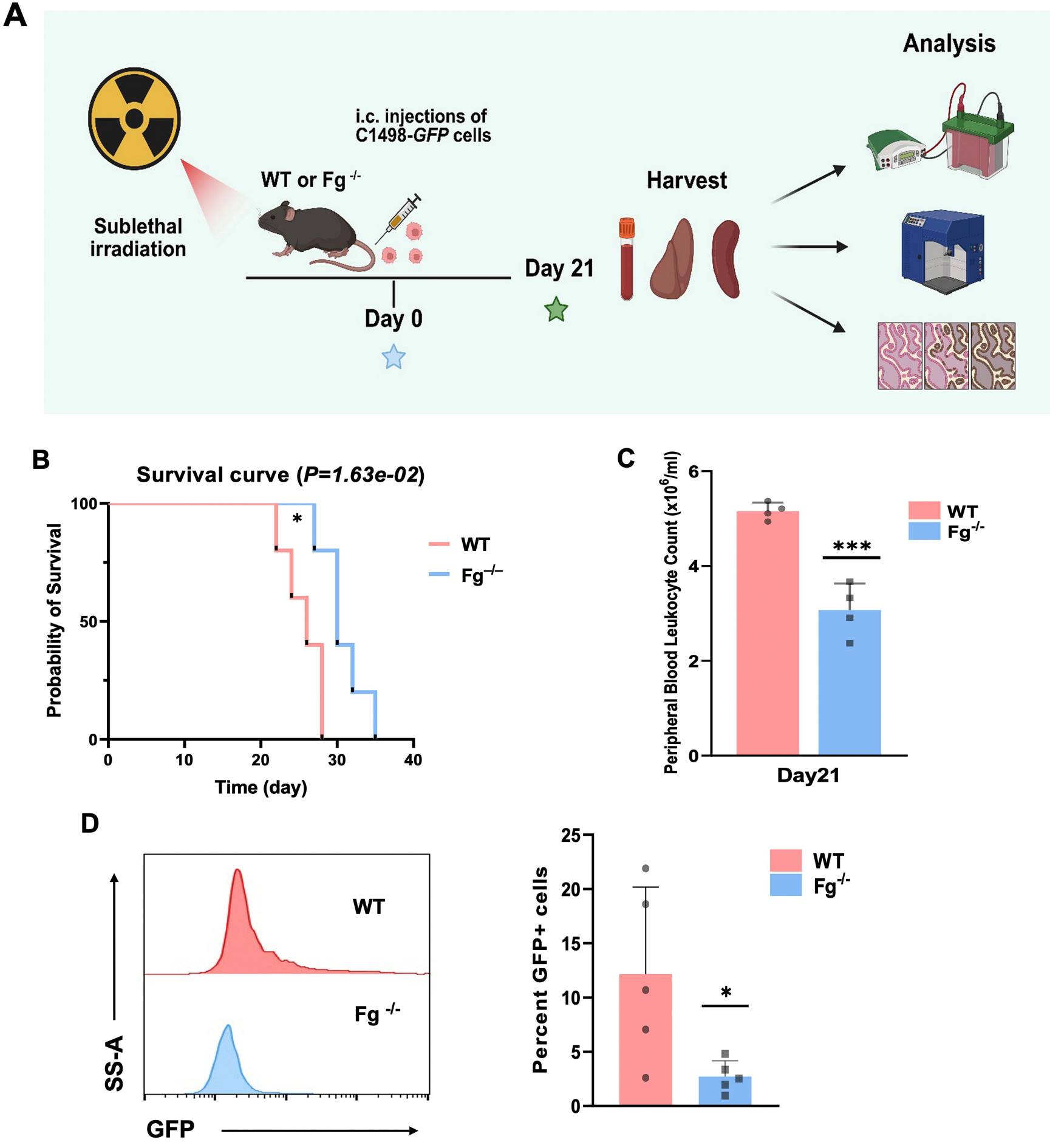
A
Analysis
i.c. injections of
C1498-GFP cells
WT or Fg -/-
Sublethal
irradiation
Harvest
Day 21
Day 0
B
Survival curve (P=1.63e-02)
Probability of Survival
100
50
0
*
WT
Fg-/-
0
10
20
30
40
Time (day)
C
Peripheral Blood Leukocyte Count (x10^6/ml)
6
4
2
0
***
WT
Fg-/-
Day21
D
WT
Fg -/-
SS-A
GFP
Percent GFP+ cells
25
20
15
10
5
0
*
WT
Fg-/-

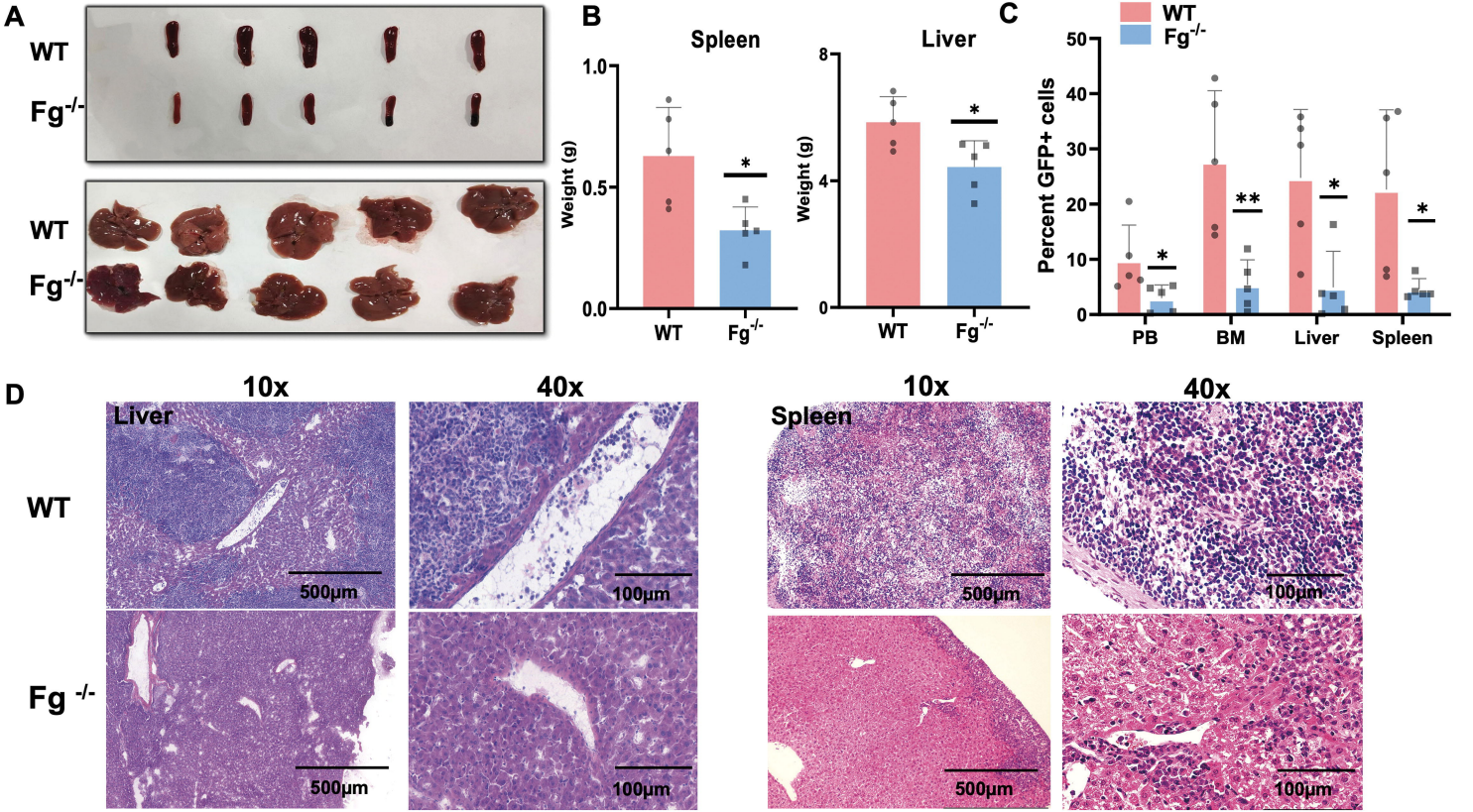
A
WT
Fg-/-
WT
Fg-/-
B
Spleen
Weight (g)
1.0
0.5
0.0
WT
Fg-/-
Liver
Weight (g)
8
4
0
WT
Fg-/-
C
WT
Fg-/-
Percent GFP+ cells
50
40
30
20
10
0
PB
BM
Liver
Spleen
D
10x
40x
Liver
WT
Fg -/-
500μm
100μm
10x
40x
Spleen
500μm
100μm

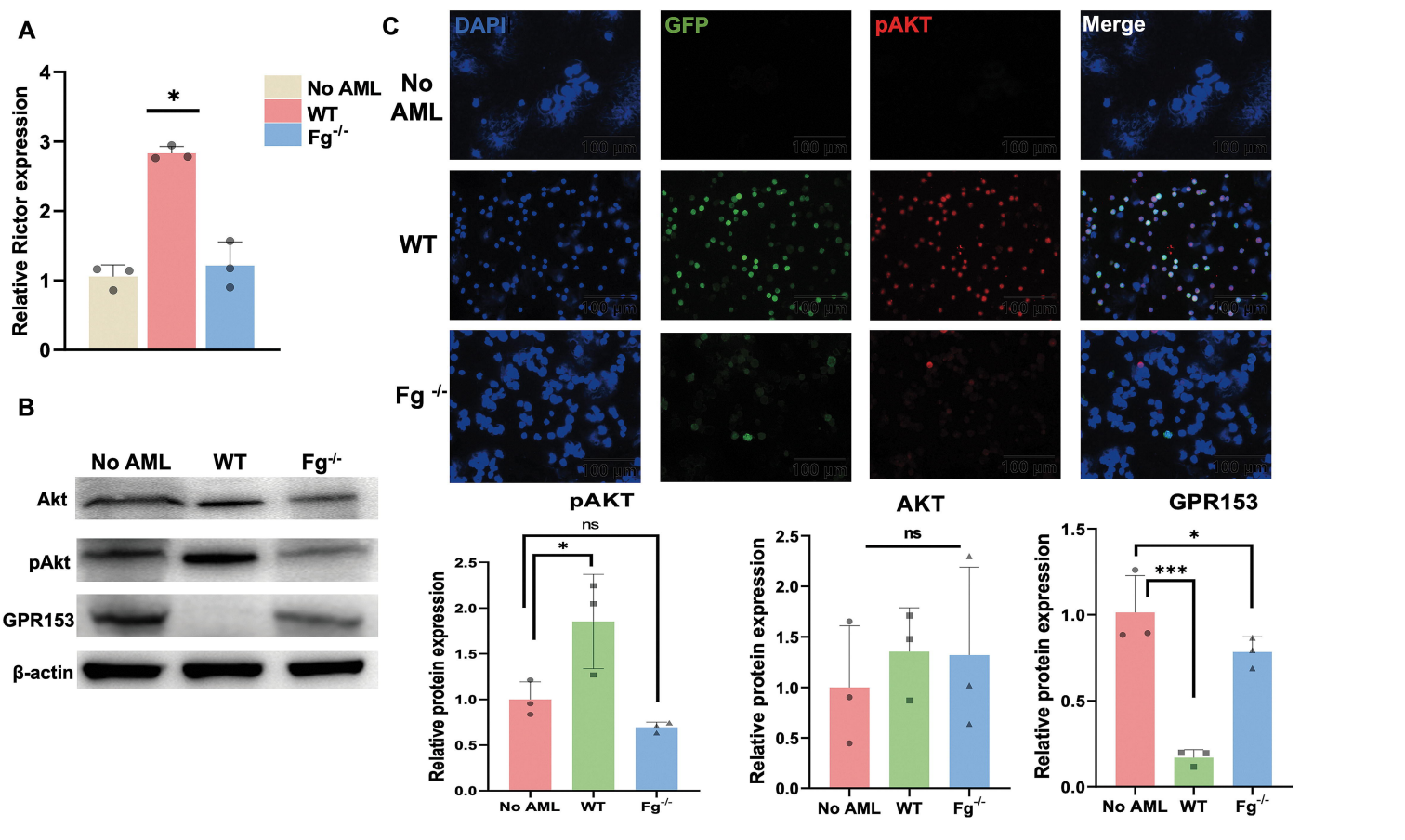
A
Relative Rictor expression
No AML
WT
Fg-/-
*
B
No AML
WT
Fg-/-
Akt
pAkt
GPR153
β-actin
C
DAPI
GFP
pAKT
Merge
No AML
WT
Fg -/-
100 μm
pAKT
ns
*
Relative protein expression
AKT
ns
GPR153
*
***

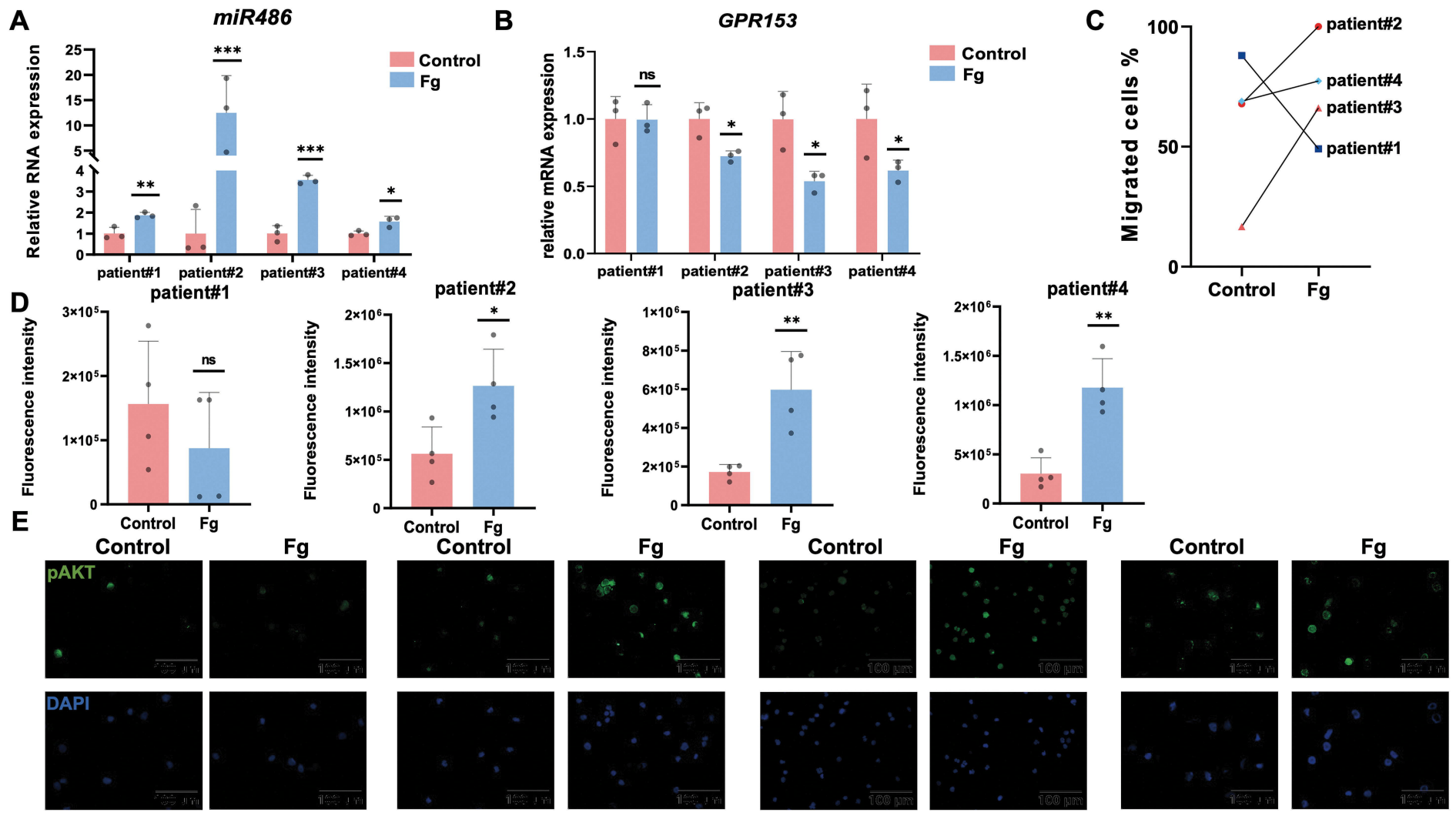
A
miR486
Relative RNA expression
Control
Fg
patient#1
patient#2
patient#3
patient#4
B
GPR153
relative mRNA expression
ns
C
Migrated cells %
patient#2
patient#4
patient#3
patient#1
Control
Fg
D
patient#1
patient#2
patient#3
patient#4
Fluorescence intensity
E
Control
Fg
pAKT
DAPI

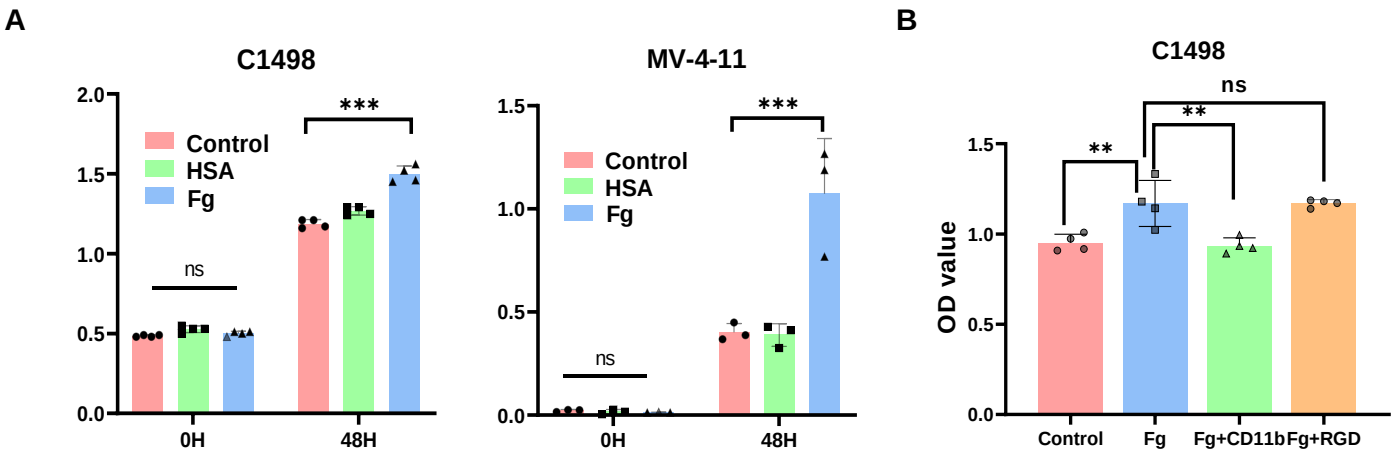

Supplementary Figure 1. Fibrinogen promotes AML cell proliferation via integrin **α**M**β**2 (A) 3g/L Fg promoted the proliferation of C1498, and MV-4-11 cells, as evaluated by CCK-8 assay (***p<0.001; ns , not significant). (B) C1498 cells were pre-incubated with a blocking antibody against CD11b (integrin αM β2) or with an RGD peptide prior to 3g/L Fg treatment. Cell proliferation was assessed at 48h.

A

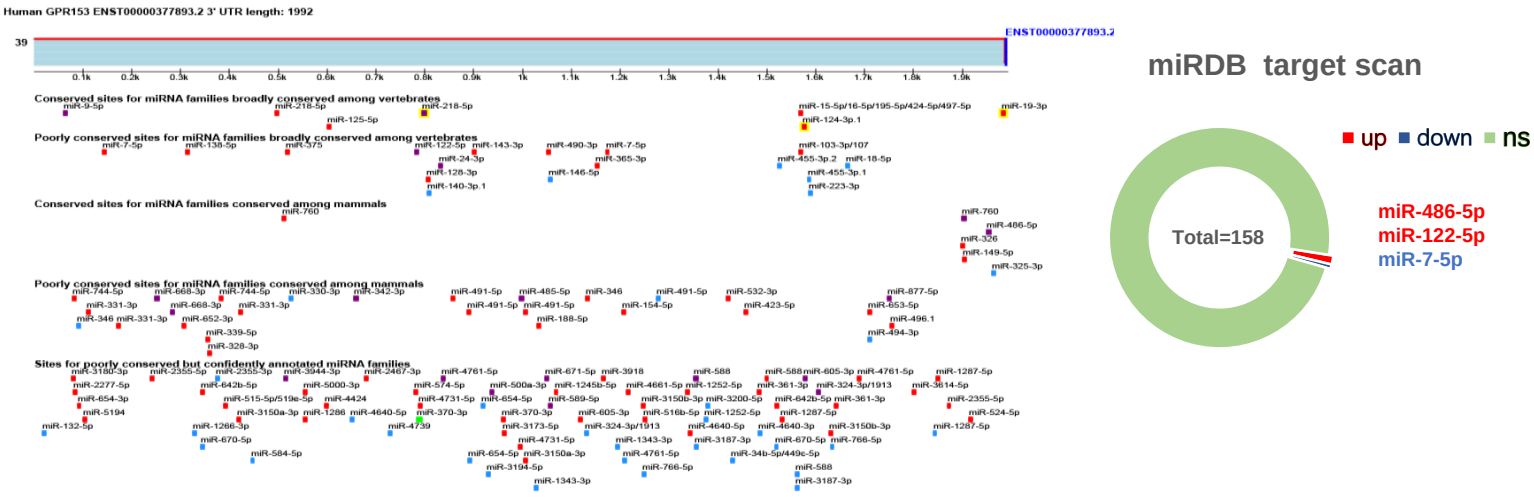

B

GAGCCCCGUCGAGUCAUGUCCU miR-486-5p 3'-5'

GAGCAUUUCUCUUCUGUACAGGA GPR153 3'UTR 5'-3'

GAGCAUUUCUCUUCUGUAGCAGGA Mut GPR153 3'UTR 5'-3'

Supplementary Figure 2. Identification of miR-486-5p as a candidate regulator of GPR153 (A) miRNAs targeting the 3'UTR of GPR153 was predicted using TargetScanand miRDB, showing an upregulation of miR-486-5p and miR-122-5p (red), and a downregulation of miR-7-5p (blue).(B) Schematic illustration of the wild-type (WT) and mutant (MUT) 3' UTR of GPR153 which matched the seed region of miR-486-5p.

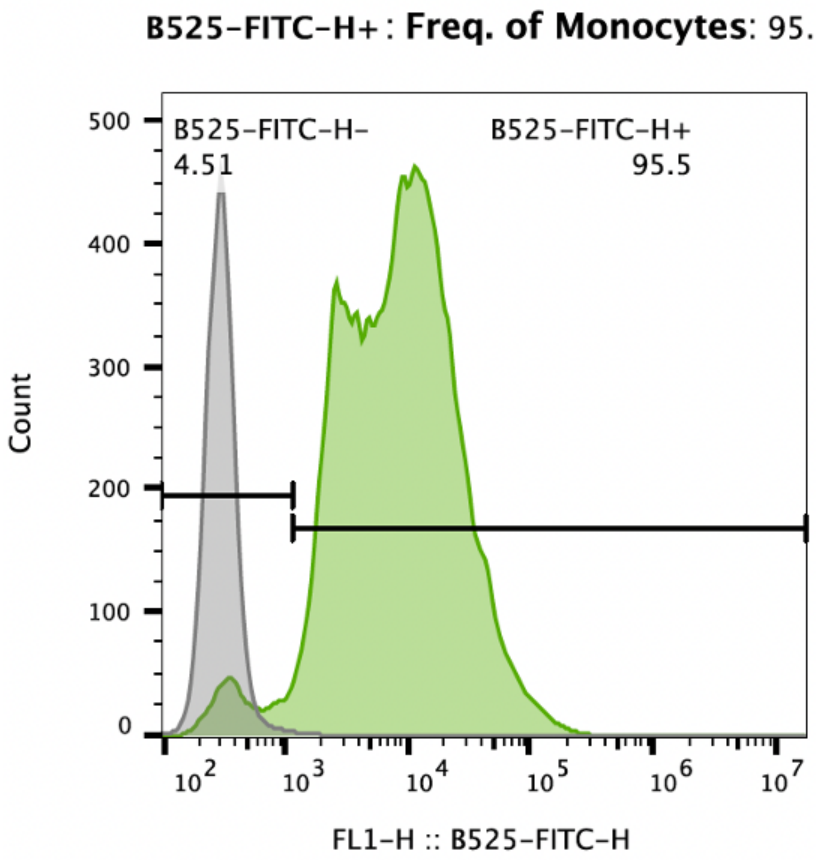

Supplementary Figure 3. Representative flow cytometry analysis of C1498 and C1498-GFP cell lines. Representative flow cytometry histograms showing GFP fluorescence intensity in C1498 cells (gray) and C1498-GFP cells (green). The C1498-GFP cell line exhibits a GFP-positive rate of ≥95%, as determined by gating on the GFP-positive population.

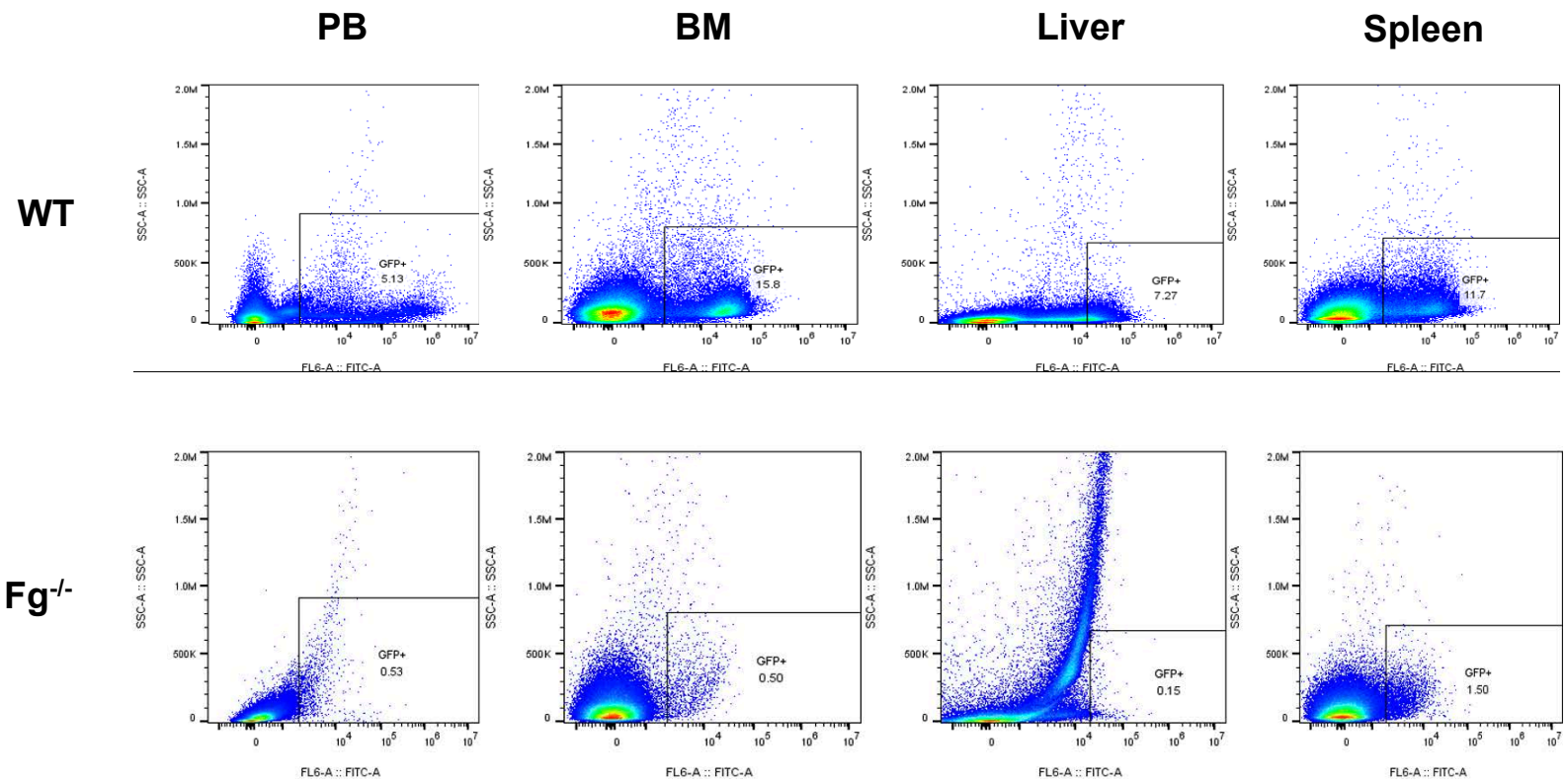

Supplementary Figure 4. Representative FACS panels of leukemia burden in peripheral blood (PB), bone marrow (BM), liver and spleen of WT and Fg -/-AML mice on day 21.

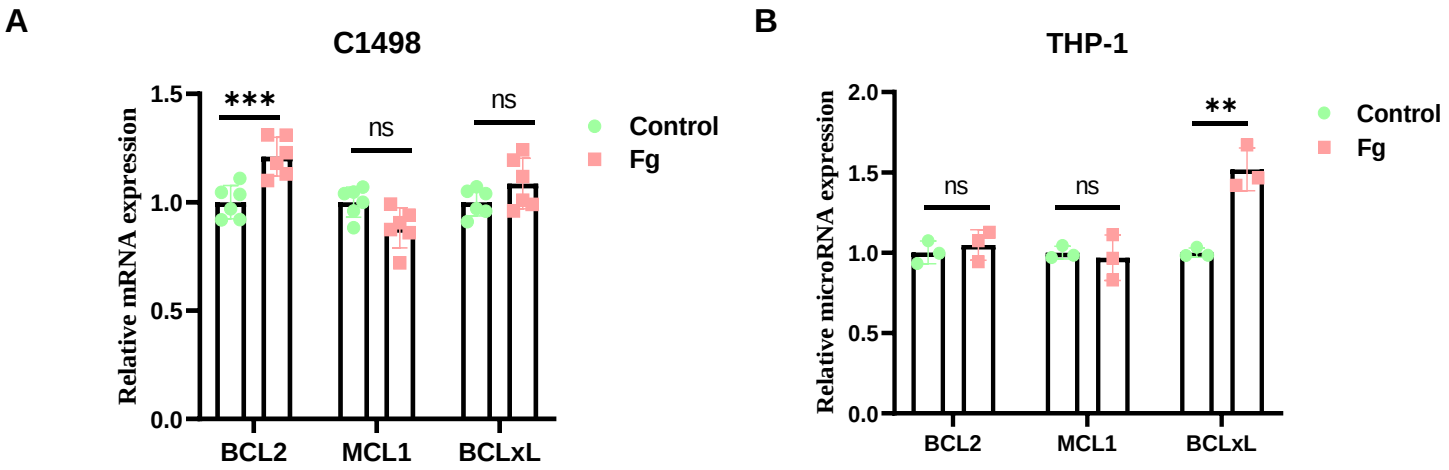

Supplementary Figure 5. Relative mRNAexpression of representative JAK/STAT downstream target genes (BCL2, MCL1, and BCL-xL) in C1498 and THP-1 cells following fibrinogen (Fg) treatment. Gene expression levels were quantified by qRT-PCR and normalized to the corresponding control group. Data are presented as mean ±SEM with individual data points shown. Statistical significance is indicated as **P < 0.01, ***P < 0.001; ns, not significant.

Table S1. Patient characteristics

Patient No.	Age	Sex	WBC 10^9/L[a]	Blasts (%) in PB	Blasts (%) in BM	Category[b]	Molecular Markers	Cytogenetics	extramedullary infiltration
1	81	M	4.73	51	25	AML with maturation	WT1 SRSF2 RUNX1 STAG2 ASXL2 CUX1	46, XY	None
2	70	M	108.57	70	60.5	Acute monoblastic/monocytic leukemia	TET2 SRSF2	Normal	Splenomegaly Hepatomegaly
3	71	M	12.25	83	97.5	Acute myelomonocytic leukemia	Flt3 ITD NPMI WT1 SETBP1 HOX11	Normal	Lymphadenopathy
4	71	F	117.57	97	98.5	AML without maturation	Flt3 ITD NPMI WT1 TET2	Normal	None

F, female; M, male; PB, peripheral blood; BM, bone marrow; WBC, white blood cell; Flt3 ITD, Flt3 internal-tandem duplication; NPM1, nucleophosmin; WT1, Wilms tumor 1; SRSF2, Serine/arginine-rich splicing factor 2; RUNX1, RUNX Family Transcription Factor 1; STAG2, stromal antigen 2; ASXL2, ASXL Transcriptional Regulator 2; CUX1, Cut-like homeobox 1; TET2, Tet methylcytosine dioxygenase 2; SETBP1, SET binding protein 1; HOX11, T-cell leukemia homeobox protein 1.

[a]Normal range is 4.5-11.0.

[b]AML categories according to the World Health Organization (WHO) classification.